



Contents lists available at ScienceDirect

Optik

journal homepage: [www.elsevier.com/locate/ijleo](http://www.elsevier.com/locate/ijleo)

Original research article

# Characterization, optical and nonlinear optical properties of TAZ organic material

Emine Babur Sas

Department of Electronics and Automation, Ahi Evran University, 40100 Kırşehir, Turkey

## ARTICLE INFO

### Keywords:

TAZ  
Optical parameters  
Opto-electronic  
Optical band gap  
HOMO-LUMO

## ABSTRACT

Since organic materials have applications in many fields, characterization and optical parameters of 3-(Biphenyl-4-yl)-5-(4-tert-butylphenyl)-4-phenyl-4H-1,2,4-triazole (TAZ) molecule have been investigated in different solvents. First, UV-vis spectra and optical parameters such as mass extinction coefficient ( $\alpha_{mass}$ ), optical band gap ( $E_g$ ), refractive index ( $n$ ), optical and electrical conductance values have been also researched as experimental and theoretical. Also the most stable state, frontier molecular orbitals and Non-linear optical properties have been investigated with DFT methods and HOMO-LUMO energy range of TAZ molecule have been compared experimentally to the optical band gap. According to the results, it was seen that the TAZ material was suitable for opto-electronic applications because of its high refractive index and wide  $E_g$  value.

## 1. Introduction

The high efficiency of OLEDs with a simple structure has always been of great importance, for example by optics, electronics and optoelectronics, because of the wide range of applications [1–9]. The materials designed for OLEDs are expected to have the appropriate HOMO-LUMO energy level, balanced charge bearing mobility, high luminescence efficiency and good stability [10–12]. The ability to carry the holes of organic materials is better than the ability to carry electrons. Therefore, it is necessary to give electron transport materials (ETMs) with high electron injection and carrying capacity to increase the performance of OLED [13]. Kido et al. developed a highly conductive layer (ETL) by co-evaporating the alkali metals together to obtain an effective electron injection and transfer in OLEDs [14].

The triazole derivatives are used quite effectively in the field of pharmaceutical chemistry [15]. 1,2,3 triazole, one of the triazole derivatives, was used for anticancer, antimicrobial and anti tuberculosis activities [14–18]. In addition, the 1,2,3-triazole group is highly stable and has been used in broad therapeutic applications such as antibacterial, antiallergic and anti-HIV [19–29]. 3-(Biphenyl-4-yl)-5-(4-tert-butylphenyl)-4-phenyl-4H-1,2,4-triazole (TAZ), which is a triazole derivative having 4 phenyl rings and a triazole core, is commonly used as ETM due to high electron injection. TAZ, which has a structure very similar to 2-(4-Biphenyl)-5-phenyl-1,3,4-oxadiazole, has been shown to have more effective electron injection and more hole blocker [30].

In this paper, we have investigated for OLED applications, spectroscopic properties and electronic structure of TAZ as an organic material. Firstly, we have calculated the potential energy surface (PES) to find the lowest-energy (lowest frequency) state of the molecule. After the optimized structure of the title molecule is found in the gas phase, the minimum energy state in DCM and chloroform solvents have been calculated. Then, the spectroscopic properties (IR and Raman) of the studied molecule have been characterized by DFT method and experimental data. Then, Uv-vis spectra have been examined experimentally and theoretically on

E-mail addresses: [baburemine@gmail.com](mailto:baburemine@gmail.com), [ebzas@ahievran.edu.tr](mailto:ebzas@ahievran.edu.tr).

<https://doi.org/10.1016/j.ijleo.2019.04.049>

Received 8 February 2019; Received in revised form 27 March 2019; Accepted 9 April 2019  
0030-4026/ © 2019 Elsevier GmbH. All rights reserved.

different solvents and found in the experimental Uv–vis spectra data mass extinction coefficient ( $\alpha_{mass}$ ), optical band gap ( $E_g$ ), refractive index ( $n$ ), optical and electrical conductance values. Furthermore, electronic properties of TAZ molecule such as frontier molecular orbital have been examined using density functional theory. Frontier molecular orbital energy gap values have been calculated TD/B3LYP and TD/CAM-B3LYP methods. Later, density of state (DOS) spectra was obtained Gausssum 2.2 program [31].

## 2. Experimental details

Chloroform and Dichloromethane (DCM) solvents and 3-(Biphenyl-4-yl)-5-(4-tert-butylphenyl)-4-phenyl-4H-1,2,4-triazole(TAZ) were purchased from a chemical company (Sigma-Aldrich, USA). FT-IR and FT-Raman spectra was taken using Perkin Elmer Spectrum Two (UATR) IR spectrophotometer and Thermo Scientific Nicolet 6700 FT-IR / NXR FT-Raman Modul instrument, respectively. The spectra was recorded from 4000 to 400  $\text{cm}^{-1}$  and from 4000 to 0  $\text{cm}^{-1}$ . Was prepared in two solvents for the TAZ molecules (DCM and chloroform) and for 0.03 mM dissolved in 10 ml. Thereafter, we taken UV-spectra values using a Genesys 10S UV–vis Spectrophotometer (Thermo Scientific).

## 3. Computational details

Spectroscopic, electronic structure and optic properties of TAZ molecule have been obtained using DFT/B3LYP method and 6–311 G(d,p) basis set [32–34]. UV-VIS and HOMO-LUMO analysis calculations were also calculated with B3LYP as well as CAM-B3LYP in order to understand the evoked condition analysis [35,36]. We have been used GAUSSIAN09 program package in the calculations [37]. In order to draw DOS diagrams, GaussSum 2.2 program have been used by running log files calculated in GAUSSIAN09 program package. Potential energy surface (PES) have been used to find the most stable structure without any symmetry. Once the molecule is optimized the spectroscopic and electronic properties was calculated. Spectroscopic properties of TAZ have been obtained by using B3LYP/6–311 G(d,p) level. Electronic and optical properties have been obtained by TD method.

## 4. Results and discussion

### 4.1. UV spectra analysis for different solvents

Uv-Vis spectrum of the TAZ molecule were examined experimentally and theoretically (for B3LYP and CAM-B3LYP functional) using different solvents. The experimental absorbance and theoretical molar absorption spectra depends on the wavelength are given in Fig. 1a, b for chloroform and DCM. As shown in Fig. 1a, two peaks are observed in both theoretical and experimental results for DCM solution. The maximum peaks of experimental and theoretical (in B3LYP and CAM-B3LYP) in this solvent are found 288, 312 and 193 nm, respectively. Similarly, in Fig. 1b the spectrums have one peaks and a shoulder. The maximum peaks 287 (experimental), 311(B3LYP) and 194 (CAM-B3LYP) nm are also observed. As shown in Fig. 1ab, the peaks in the theoretical and experimental spectrums calculations are found to be approximately the same for both solvents. However, different values were observed for different solutions in experimental results. The energy values corresponding to the maximum peaks in the experimental Uv–vis spectra are 4.30 and 4.32 eV for DCM and chloroform solvent, respectively.

### 4.2. Optical parameters of the TAZ

Optical absorption measurements are one of the most common techniques used to determine the direct and indirect energy ranges, optical absorption coefficient, and band structure of the sample studied. We've achieved some optical parameters for the TAZ molecule such as mass extinction coefficient ( $\alpha_{mass}$ ), optical band gap ( $E_g$ ), refractive index ( $n$ ), optical and electrical conductance values in this context for different solvents.

The  $\alpha_{mass}$  coefficient is an important parameter for optoelectronic applications. We obtained the  $\alpha_{mass}$  values of the TAZ molecule solutions for DCM and chloroform and their graphs are given in Fig. 2 [38–41]. The molecular weight ( $M_A$ ) of the TAZ molecule used

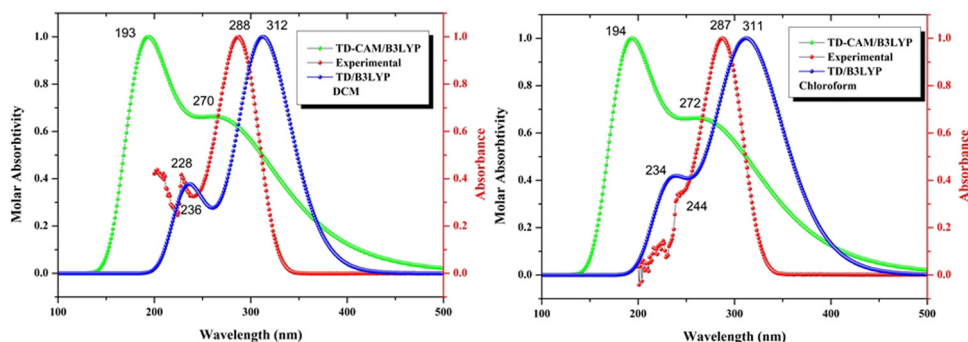


Fig. 1. The experimental and theoretical molar absorptivity plots vs. wavelength ( $\lambda$ ) of TAZ for DCM and chloroform solvents.

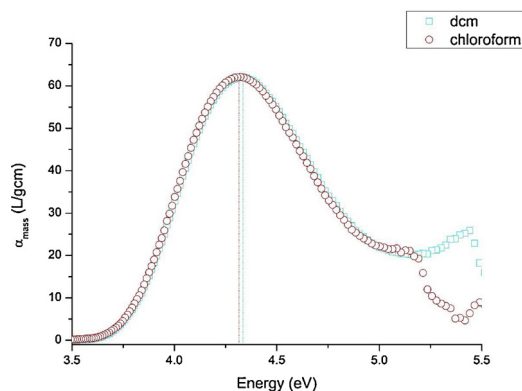


Fig. 2. The mass extinction coefficient ( $\alpha_{mass}$ ) plot vs wavelength ( $\lambda$ ) of TAZ for DCM and chloroform solvents.

in these calculations is 425,569 g/mol. As can be seen from the Fig. 2, the mass extinction coefficient (4.33 eV) of the TAZ molecule in the DCM solvent is greater than the value in the chloroform (4.31 eV) solvent.

Forbidden energy band intervals using optical transmittance spectra can be calculated. The absorption coefficients ( $\alpha$ ) of each wavelength are calculated using Beer Lambert's law. When absorption coefficients ( $\alpha$ ) are found, the forbidden energy band gap can be calculated using the Tauc equation [42]:

$$\alpha E = B(E - E_g)^p \quad (1)$$

where  $E$  are the photon energy,  $B$  is a constant and  $p$  is a unitless constant with a value of 1/2 for direct transitions and 2 for indirect transitions. For TAZ semiconductor, the appropriate value of the  $p$  was found to be 1/2, that is, for electrical dipole allowed direct band gap transitions. Thus, the  $(\alpha E)^2$  curves vs.  $E$  of the TAZ for chloroform and DCM were indicated in Fig. 3. The allowed direct band gap ( $E_g$ ) values were obtained from the linear regions of Fig. 3. The optical band gap ( $E_g$ ) of the TAZ molecule according to Fig. 3 was found to be 3.92 and 3.91 eV for DCM and chloroform, respectively. The  $E_g$  value was found for the same solvents using the methods of TD/B3LYP and CAM/B3LYP. The results obtained with TD/B3LYP method are consistent with the experimental results and with the absorbance band edge calculated while the  $E_g$  range is found.

Some other optical properties such as refractive index of the of TAZ molecule were studied. The refractive index ( $n$ ) is an important optical parameter. It is known that the  $n$  value of a material decreases with energy gap. The refractive index of the molecule are calculated using reflectance and extinction coefficient ( $k$ ) data [43]. The refractive index graph for the TAZ molecule is given in Fig. 4 for different solvents. The value of  $n$  was found to be different for DCM and chloroform solvents and gave the highest value in the DCM solvent from these solvents. This value decreases with increasing wavelength. According to Fig. 4, the refractive index for TAZ is 2.64 and 2.62 (3.97 eV). The refractive index is reduced to the minimum 1.018 and 0.755 and is 3.52 eV.

Another parameter for optical materials is the optical conductance ( $\sigma_{opt}$ ) and electrical conductance ( $\sigma_{elct}$ ) [44]. These parameters depend on absorption coefficients ( $\alpha$ ), refractive index ( $n$ ), speed of light ( $c$ ) and wavelength  $\lambda$ . The energy dependent graphs of the optical conductance and electrical conductance values for the TAZ molecule are given in Fig. 5a–b for DCM and chloroform solvent. As can be seen in Fig. 5a, the optical conductance the maximum value is seen in the chloroform solvent at 4.11 eV. Similarly, electrical conductance chloroform solvent gave the maximum peak (3.95 eV) in Fig. 5b. These results indicate that this parameter value can be changed in solvent environments.

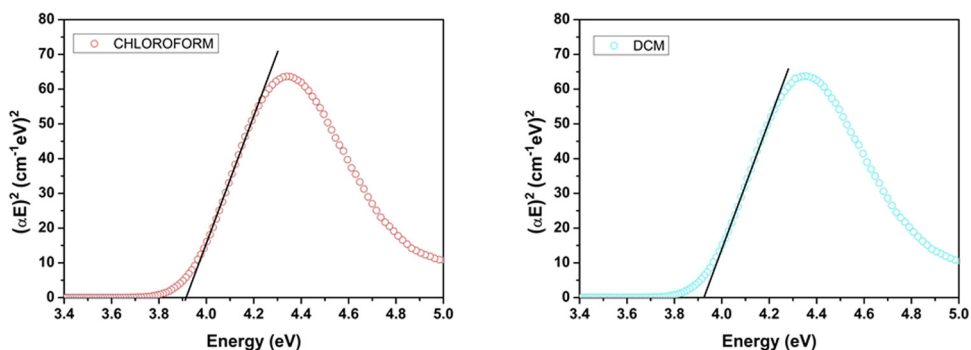


Fig. 3. The  $(\alpha h\nu)^2$  vs photon energy ( $E$ ) of TAZ for DCM and chloroform solvents.

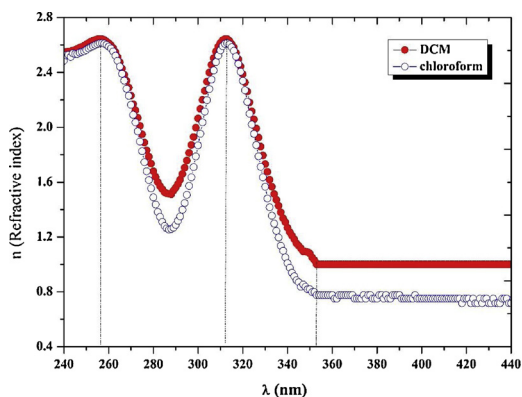


Fig. 4. The refractive index ( $n$ ) curves wavelength ( $\lambda$ ) of TAZ for DCM and chloroform solvents.

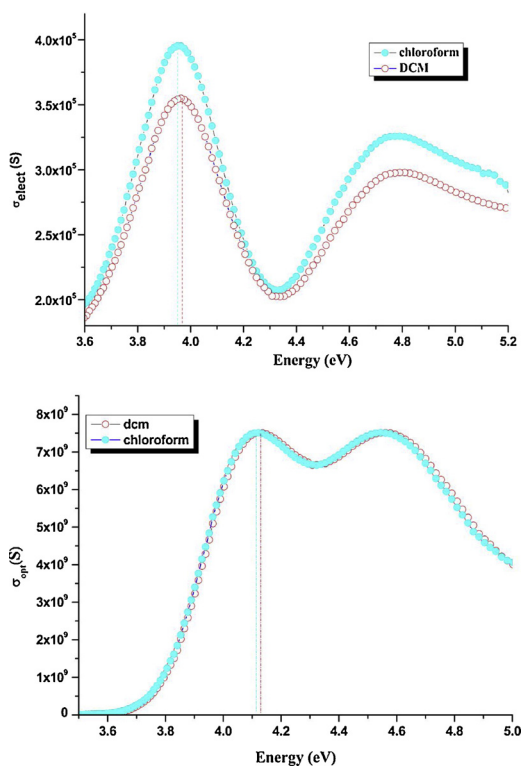


Fig. 5. a) The optical conductance ( $\sigma_{opt}$ ) and b) electrical conductance ( $\sigma_{elect}$ ) curves vs. ( $E$ ) of TAZ for DCM and chloroform solvents.

#### 4.3. Potential energy surface (PES) and structural and vibrational analysis

PES was calculated to find the lowest energy state of the TAZ molecule on single bonds that were thought to alter this energy. The all phenyl rings attached to the triazole ring are calculated as 36 steps by varying  $10^\circ$  in the range  $0-360^\circ$ . The calculated 5 torsion angles for the molecule. These angles are C5-C2-C6-C8, C9-C13-C16-C18, C4-C1-C38-C40, C43-C45-C48-C57 and C2-N3-C27-C28, respectively. Potential Energy Surfaces (PES) for TAZ molecule are shown Fig. 6a. After finding the lowest energy state, the molecular geometry of TAZ molecule was optimized using B3LYP / 6-311 G(d,p) level and the molecular structure are given Fig. 6b. The molecule was found to be in C1 form without any force of symmetry and the lowest vibration frequency was determined as positive. The lowest frequency was found to be 16.36 (chloroform) and 16.53 (DCM) when the optimized structure was calculated on solvents. According to these results, the TAZ molecule in chloroform solvent has a more stable structure.

The TAZ molecule with empirical formula  $C_{30}H_{27}N_3$  has 60 atoms and 174 vibrational bands. The vibrational modes of the molecule are computed with DFT/B3LYP methods. The experimental and theoretical vibration spectra are shown on a single graph in Fig. 7 for comparison. In the theoretical IR spectrum the sharpest band are seen at  $1460\text{ cm}^{-1}$ . This vibrational mode is the band in which the CH3 group shows scissoring vibration. This value corresponds to  $1472\text{ cm}^{-1}$  in the experimental IR spectrum. The in-plane

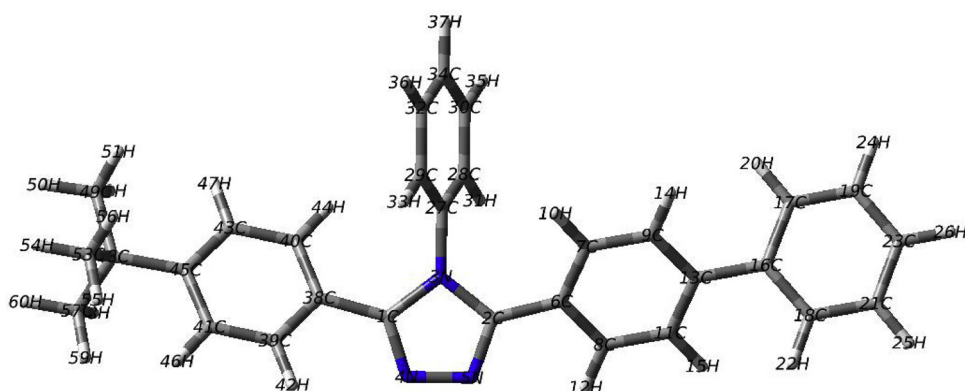
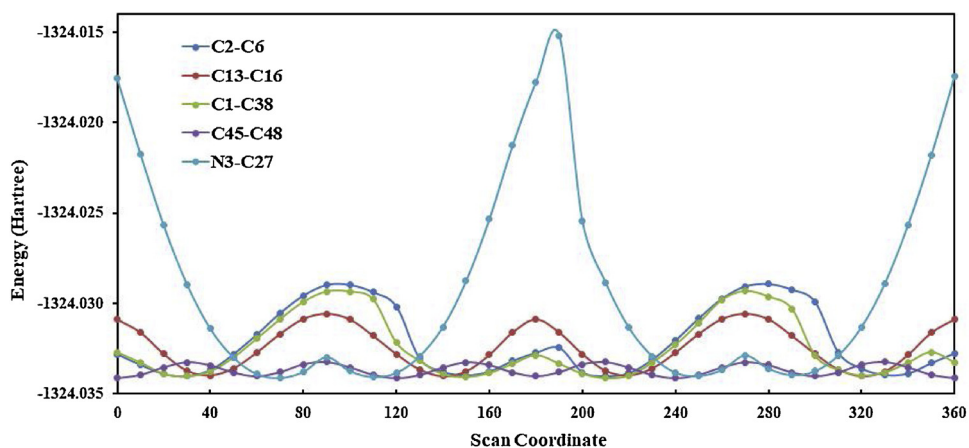


Fig. 6. a) Potential energy surface (PES) of TAZ. b) Theoretical optimized geometric structure of the TAZ.

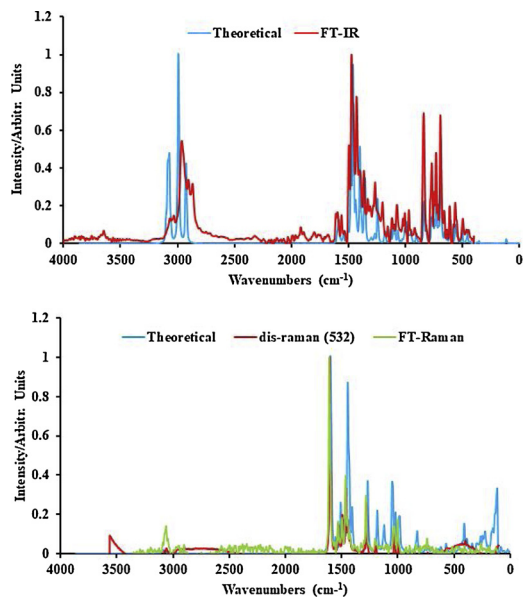


Fig. 7. The experimental and calculated (with the scale factor) FT-IR and FT-Raman spectra of the TAZ.

bending (CH) in the phenyl rings, the breathing in the triazole ring and scissoring vibrations of the  $\text{CH}_3$  groups modes are calculated as  $1440\text{ cm}^{-1}$  in which seen together are the sharpest band in the Raman spectrum. This bands are observed as  $1460$  and  $1465\text{ cm}^{-1}$  in dis-Raman and FT-Raman spectrums, respectively.

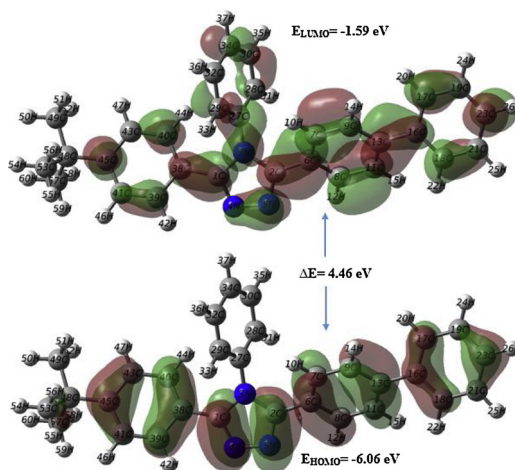


Fig. 8. The frontier molecular orbitals of the TAZ for chloroform solvent.

#### 4.4. Frontier molecular orbitals and total density of states (DOS)

In order to understand the nature of the charge transfer in the compounds, we have drawn the most important transition of the TAZ molecule in Fig. 8. This transition is between the lowest unoccupied molecular orbital (LUMO) and the highest occupied molecular orbital (HOMO), and these orbitals are called frontier molecular orbitals. This HOMO and LUMO orbitals of the molecule in which the transition between orbitals found to be concentrated in the group of atoms, and gives important information about the characteristic of intramolecular charge transfer [45]. The valence band (HOMO) in the TAZ molecule was localized only in the triazole groups and three phenyl groups while the conductivity band (LUMO) was localized the whole of molecule except C-3(CH<sub>3</sub>) groups. The energy difference between the frontier molecular orbitals is an important parameter for conductivity [48,49]. This energy difference was calculated as 4.46 and 4.47 eV for the TAZ molecule in TD-DFT/B3LYP method and as 6.93 and 6.94 eV in TD-DFT/CAM-B3LYP method for chloroform and DMF solvent respectively. In gas phase, these values were calculated as 3.64 eV. The Eg (optical band gap) value measured experimentally was found as 3.92 eV in DCM solvent and as 3.91 eV in the chloroform solvent. The lower optical band gap of the TAZ is obtained for chloroform solvent.

Taking account of only the HOMO-LUMO orbitals may not give a real definition [46]. In this case, neighboring orbitals also can use characterization of frontier orbitals. Therefore, the total density of states (DOS) [47–51] were computed and created by convoluting the molecular orbital information with Gaussian curves of unit height and the full width at half maximum of 0.3 eV using GaussSum 2.2 program [31] In the B3LYP and CAM method, the HOMO-LUMO energy band gap calculated in chloroform and DCM solvents was combined with the Eg (optic band gap) which were experimentally used in the same solvents using Tauc formula and DOS diagram to form Fig. 9. According to this diagram, the B3LYP method gives better results compared to the experimentally available Eg (optical band gap) value.

#### 4.5. Nonlinear optical properties and dipole moment

Values such as polarizability and hyperpolarizability are defined as non-linear optical properties of molecules. Finding data gives clues that the materials can be used in areas such as optical sensors, optical switching, signal processing and displays. Theoretical studies have an important place in finding the non-linear optical properties of materials. In this study, non-linear optical properties of TAZ molecule such as polarizability ( $\alpha$ ), anisotropy of polarizability ( $\Delta\alpha$ ), and mean molecular hyperpolarizability ( $\beta$ ) and total dipole moment were examined by DFT/B3LYP methods and given in Table 1. In order to find non-linear optical values, Gaussian output file was used and atomic units in output file were converted to electronic units. These values must be large in order for a material to show good NLO properties. The values obtained are generally compared to urea, which is a polarized molecule. These values for TAZ are calculated as  $\beta_{\text{tot}} = 9409.616571 \times 10^{-33}$  esu and  $\Delta\alpha = 162.458717 \times 10^{-24}$  esu. When the results are compared with urea ( $\beta_{\text{tot}} = 194.7 \times 10^{-33}$  esu and  $\Delta\alpha = 3.8312 \times 10^{-24}$  esu), it is seen that the values are approximately 100 times higher than urea, and these results indicate that TAZ can be used as NLO material.

When the dipole moment of the TAZ molecule was examined in different solvents, a high value such as polarizability and hyperpolarizability was found. These values are 5.8635 Debye in the gas phase, 7.9709 Debye in DCM solvent and 7.5839 Debye in chloroform. The highest contribution to these dipole moments is provided by  $\mu_y$  ( $\mu_y = 5.8514$  Debye). These values in the solvents and gas phase are compatible with Eg (optical band gap) values.

## 5. Conclusions

Some physical and chemical properties of the TAZ molecule in DCM, chloroform solvents and in the gas phase (such as

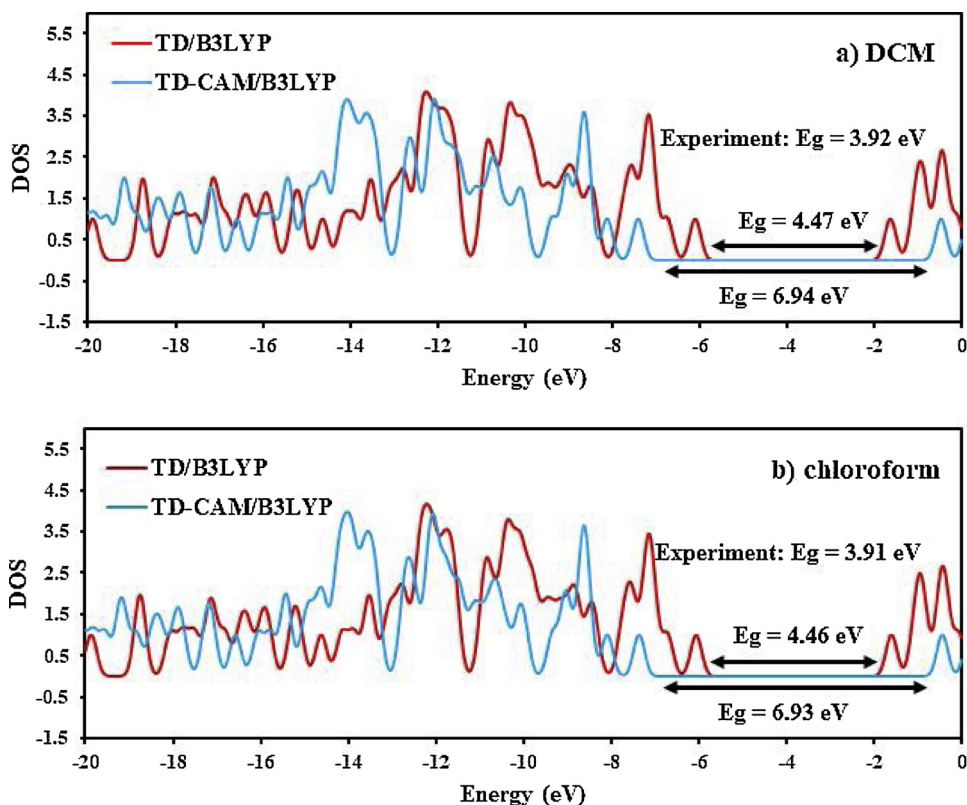


Fig. 9. Density of state (DOS) spectrum of TAZ.

Table 1

The dipole moments  $\mu$  (D), the polarizability  $\alpha$  (a.u.), the average polarizability  $\alpha_0$  ( $\times 10^{-24}$  esu), the anisotropy of the polarizability  $\Delta\alpha$  ( $\times 10^{-24}$  esu), and the first hyperpolarizability  $\beta$  ( $\times 10^{-33}$  esu) of TAZ.

$\mu_x$	-0.3651	$\beta_{xxx}$	5607.1982
$\mu_y$	5.8514	$\beta_{xxy}$	4096.0322
$\mu_z$	0.0951	$\beta_{xyy}$	33.4556
$\mu_0$	5.863550459	$\beta_{yyy}$	2805.1546
$\alpha_{xx}$	89.023672	$\beta_{xxx}$	189.5495
$\alpha_{xy}$	0.893692	$\beta_{xyz}$	157.6282
$\alpha_{yy}$	50.020746	$\beta_{yyz}$	205.8152
$\alpha_{xz}$	-2.246597	$\beta_{xzz}$	385.4514
$\alpha_{yz}$	-0.382304	$\beta_{yzz}$	323.8527
$\alpha_{zz}$	31.099935	$\beta_{zzz}$	-234.9148
$\alpha_{total}$	56.714784	$\beta_x$	6026.105201
$\Delta\alpha$	162.458717	$\beta_y$	7225.039511
		$\beta_z$	160.4499539
		$\beta$	9409.616571

spectroscopic, electronic, photophysical) were investigated. Compared to the vibrational spectra of the two different solvents and gas phase spectroscopically examined the molecule, it was found that the chloroform solvent (16.36) was more stable than DCM (16.53). In order to examine the advantages of the molecule in optoelectronic applications, band gap was compared theoretically and experimentally and B3LYP method was found to be better than CAM/B3LYP method. TAZ has a wide range of optical band gap (3.6 eV) and a high refractive index ( $n \sim 2.6$ ) as a semiconductor. Due to these properties, it can be used in optoelectronic applications.

#### Acknowledgements

This work was supported by Ahi Evran University Scientific Project Unit (BAP) with, Project No: TBY.A3.17.004.

#### References

- [1] Y. Sun, N.C. Giebink, H. Kanno, B. Ma, M.E. Thompson, S.R. Forrest, *Nature* 440 (2006) 908.

- [2] J. Lee, W.J. Sung, C.W. Joo, H. Cho, N.S. Cho, G.-W. Lee, D.-H. Hwang, J.-I. Lee, ETRI J 38 (2016) 260.
- [3] B. Zhang, G. Tan, C.S. Lam, B. Yao, C.L. Ho, L. Liu, Z. Xie, W.Y. Wong, J. Ding, L. Wang, Adv. Mater. 24 (2012) 1873.
- [4] S. Reineke, F. Linder, G. Schwartz, N. Seidler, K. Walzner, B. Lüssem, K. Leo, Nature 459 (2009) 234.
- [5] E.B. Sas, M. Kurban, B. Gündüz, M. Kurt, Photophysical, spectroscopic properties and electronic structure of BND: experiment and theory, Synth. Met. 246 (2018) 39–44.
- [6] F. So, J. Kido, P. Burrows, MRS Bull. 33 (2008) 663.
- [7] E. Taniş, E.B. Sas, B. Gündüz, M. Kurt, Required theoretical and experimental physical characteristics of tris[4-(diethylamino)phenyl] amine organic material, J. Mater. Sci. Mater. Electron. 29 (2018) 16111–16119.
- [8] T. Nakayama, K. Hiyama, K. Furukawa, H. Ohtani, SID 16 (2008) 231.
- [9] A. Ltaief, A. Bouazizi, J. Davenas, R. Ben Chaabane, H. Ben Ouada, Synth. Met. 147 (2004) 261.
- [10] J. Chen, X. Chen, Z. Yang, Z. Chi, Z. Yang, Y. Zhang, J. Xu, Z. Chi, M.P. Aldred, J. Mater. Chem. C6 (2018) 3226.
- [11] P. Bujak, I.K.-Bajer, M. Zagorska, V. Maurel, I. Wielgus, A. Pron, Chem. Soc. Rev. 42 (2013) 8895.
- [12] M. Kurban, B. Gündüz, J. Mol. Struct. 1137 (2017) 403.
- [13] S.-J. Su, T. Chiba, T. Takeda, J. Kido, Adv. Mater. 20 (2008) 2125.
- [14] J. Kido, T. Matsumoto, Appl. Phys. Lett. 73 (1998) 2866.
- [15] Pinki Yadav, Kashmiri Lal, Lokesh Kumar, Ashwani Kumar, et al., Synthesis, crystal structure and antimicrobial potential of some fluorinated chalcone-1,2,3-triazole conjugates, Eur. J. Med. Chem. 155 (2018) 263–274.
- [16] Y.C. Duan, Y.C. Zheng, X.C. Li, M.M. Wang, et al., Design, synthesis and antiproliferative activity studies of novel 1,2,3-triazole-dithiocarbamate-urea hybrids, Eur. J. Med. Chem. 64 (2013) 99–110.
- [17] K. Lal, P. Yadav, A. Kumar, A. Kumar, A.K. Paul, Design, synthesis, characterization, antimicrobial evaluation and molecular modeling studies of some dehydroacetic acid-chalcone-1,2,3-triazole hybrids, Bioorg. Chem. 17 (2018) 236–244.
- [18] C. Gill, G. Jadhav, M. Shaikh, R. Kale, A. Ghawalkar, D. Nagargoje, M. Shiradkar, Clubbed [1,2,3] triazoles by fluorine benzimidazole: a novel approach to H37Rv inhibitors as a potential treatment for tuberculosis, Bioorg. Med. Chem. Lett. 18 (2008) 6244–6247.
- [19] N.S. Vatmurge, B.G. Hazra, V.S. Pore, et al., Synthesis and antimicrobial activity of  $\beta$ -lactam–bile acid conjugates linked via triazole, Bioorg. Med. Chem. Lett. 18 (2008) 2043–2047.
- [20] E.M. Souza-Fagundes, J. Delpe, P.H.D.M. Prazeres, et al., Correlation of structural features of novel 1,2,3-triazoles with their neurotoxic and tumoricidal properties, Chem. Biol. Interact. 291 (2018) 253–263.
- [21] S. Sathish Kumar, H.P. Kavitha, Synthesis and biological applications of triazole derivatives—a review, Mini-reviews Org. Chem. 10 (2013) 40–65.
- [22] R. Pingaew, P. Mandi, C. Nantasenamat, et al., Design, synthesis and molecular docking studies of novel n-benzenesulfonyl-1,2,3,4-tetrahydroisoquinoline-based triazoles with potential anticancer activity, Eur. J. Med. Chem. 81 (2014) 192–203.
- [23] B. ShivaramaHolla, K. NarayanaPoojary, B. SooryanarayanaRao, et al., New bis amino mercapto triazoles and bis-triazolo thiazoles as possible anticancer agents, Eur. J. Med. Chem. 37 (2002) 511–517.
- [24] R. Alvarez, S. Velazquez, A. San-Felix, et al., 1,2,3-triazole-[2,5-bis-o-(tertbutyldimethylsilyl)-Beta.-d-ribofuranosyl]-3'-spiro-5'-(4'-amino-1',2'-oxathiole 2',2'-dioxide) (tsao) analogs: synthesis and anti-hiv-1 activity, J. Med. Chem. 37 (1994) 4185–4194.
- [25] R. Pingaew, S. Prachayasittikul, S. Ruchirawat, et al., Synthesis and cytotoxicity of novel 4-(4-(substituted)-1h-1,2,3-triazol-1-yl)-n-phenethylbenzenesulfonamides, Med. Chem. Res. 23 (2014) 1768–1780.
- [26] M. Kidwai, A. Jain, Regioselective synthesis of 1,4-disubstituted triazoles using bis ([I]prolinato-n,o)zn complex as an efficient catalyst in water as a sole solvent, Appl. Organomet. Chem. 25 (2011) 620–625.
- [27] V. Prachayasittikul, R. Pingaew, N. Anuwongcharoen, et al., Discovery of novel 1,2,3-triazole derivatives as anticancer agents using qsar and in silico structural modification, SpringerPlus 4 (2015) 1–22.
- [28] M.J. Genin, D.A. Allwine, D.J. Anderson, et al., Substituent effects on the antibacterial activity of nitrogen–carbon-linked (azolyphenyl) oxazolidinones with expanded activity against the fastidious gram-negative organisms Haemophilus influenzae and Moraxella catarrhalis, J. Med. Chem. 43 (2000) 953–970.
- [29] B. ShivaramaHolla, B. Veerendra, M.K. Shivananda, et al., Synthesis characterization and anticancer activity studies on some mannich bases derived from 1,2,4-triazoles, Eur. J. Med. Chem. 38 (2003) 759–767.
- [30] M.-H. Tsai, H.-W. Lin, H.-C. Su, T.-H. Ke, C.-C. Wu, F.-C. Fang, Y.-L. Liao, K.-T. Wong, C.-L. Wu, Adv. Mater. 18 (2006) 1216.
- [31] N.M. O'Boyle, A.L. Tenderholt, K.M. Langner, J. Comp. Chem. 29 (2008) 839–845.
- [32] W. Kohn, L.J. Sham, Phys. Rev. 140 (1965) A1133.
- [33] A.D. Becke, Phys. Rev. A 38 (1988) 3098.
- [34] S.H. Vosko, L. Vilk, M. Nusair, Can. J. Phys. 58 (1980) 1200.
- [35] T. Yanai, D.P. Tew, N.C. Handy, Chem. Phys. Lett. 393 (2004) 51.
- [36] M.E. Foster, B.M. Wong, J. Chem. Theory Comput. 8 (2012) 2682.
- [37] M.J. Frisch, G.W. Trucks, H.B. Schlegel, G.E. Scuseria, M.A. Robb, J.R. Cheeseman, G. Scalmani, V. Barone, B. Mennucci, G.A. Petersson, et al., Gaussian 09, Revision B.01, Gaussian, Inc., Wallingford CT, 2009.
- [38] A. Adachi, A. Kudo, T. Sakata, The optical and photoelectrochemical properties of electrodeposited CdS and SnS thin films, Bull. Chem. Soc. Jpn. 68 (1995) 3283–3288.
- [39] M. Biçer, İ. Şişman, Electrodeposition and growth mechanism of SnSe thin films, Appl. Surf. Sci. 257 (2011) 2944–2949.
- [40] İ. Şişman, Ü. Demir, Electrochemical growth and characterization of size-quantized CdTe thin films grown by under potential deposition, J. Electroanal. Chem. 651 (2011) 222–227.
- [41] İlkyay Şişman, Adil Baçoğlu, Effect of Se content on the structural, morphologica and optical properties of Bi<sub>2</sub>Te<sub>3</sub>ySe<sub>y</sub> thin films electrodeposited by under potential deposition technique, Mater. Sci. Semicond. Process. 54 (2016) 57–64.
- [42] H. Tokuhisa, M. Era, T. Tsutsui, S. Saito, Appl. Phys. Lett. 66 (1995) 3433.
- [43] Sümeyye Altürk, Davut Avcı, Adil Baçoğlu, Ömer Tamer, Yusuf Atalaya, Necmi Dege, Copper(II) complex with 6-methylpyridine-2-carboxylic acid: experimental and computational study on the XRD, FT-IR and UV–vis spectra, refractive index, band gap and NLO parameters, Spectrochim. Acta Part A: Mol. Biomol. Spectrosc. 190 (2018) 220–230.
- [44] M. Yarmohammadi, AIP Adv. 6 (2016) 85008.
- [45] E.B. Sas, M. Cevik, M. Kurt, Experimental and theoretical analysis of 2-amino 1-methyl benzimidazole molecule based on DFT, J. Mol. Struct. 1149 (2017) 882–892.
- [46] E.B. Sas, N. Cankaya, M. Kurt, Synthesis of 2-(bis(cyanomethyl)amino)-2-oxoethyl methacrylate monomer molecule and its characterization by experimental and theoretical methods, J. Mol. Struct. 1161 (2018) 433–441.
- [47] I. Fleming, Frontier Orbitals and Organic Chemical Reactions, Wiley, London, 1976.
- [48] K. Fukui, Science 218 (1982) 747–754.
- [49] R. Hoffmann, Solids and Surfaces: A Chemist's View of Bonding in Extended Structures, VCH Publishers, New York, 1988.
- [50] T. Hughbanks, R. Hoffmann, J. Am. Chem. Soc. 105 (1983) 3528.
- [51] J.G. Malecki, Polyhedron 29 (2010) 1973.